

Scanning-tunneling-microscopy study of the surface diffusion of sulfur on Re(0001)

J. C. Dunphy

*Center for Advanced Materials, Material Science Division, Lawrence Berkeley Laboratory, Berkeley, California 94720
and Department of Physics, University of California, Berkeley, Berkeley, California 94720*

P. Sautet,* D. F. Ogletree, O. Dabbousi,[†] and M. B. Salmeron

Center for Advanced Materials, Material Science Division, Lawrence Berkeley Laboratory, Berkeley, California 94720

(Received 13 May 1992; revised manuscript received 7 August 1992)

Low coverages of sulfur chemisorbed on the rhenium (0001) surface were studied by scanning tunneling microscopy (STM). At one-quarter monolayer coverage, sulfur forms a $p(2 \times 2)$ ordered overlayer, consistent with low-energy electron-diffraction results. At lower coverages, some of the sulfur forms small islands of the $p(2 \times 2)$ structure. Between the islands, sulfur atoms diffuse over the surface as a lattice gas. In our conditions, the residence time of the sulfur atoms in each site is comparable to the STM scan rate, which gives rise to an apparently noisy image. However, a spatial correlation function was used to determine that this apparent noise is due to diffusing sulfur that maintains a local $p(2 \times 2)$ order. This order is due to a weak attractive interaction between the diffusing atoms at twice the Re lattice spacing and a repulsive interaction at closer distances. The strength of the attractive interaction was measured by fitting the results of the correlation function to an Ising model of the interaction of sulfur atoms on the surface. The energy barrier to diffusion was calculated from the sulfur residence time, and compares well with an extended Hückel calculation.

I. INTRODUCTION

The study of diffusion of atoms on surfaces is an important area of surface science. A measurement of the speed of diffusion of adsorbed species on surfaces is important to the understanding of catalytic reactions. Diffusion rates also play a major role in controlling nucleation and growth on surfaces. Many methods of determining diffusion coefficients on surfaces have been developed. One method relies on measuring the change in shape of a feature on a surface that is composed of many atoms. This can be done using scanning electron microscopy (SEM) or scanning tunneling microscopy (STM) imaging.^{1,2} This method does not separate the effects of surface diffusion on terraces from kink and bulk diffusion. Several other methods that do make an independent measurement of surface diffusion are high-energy electron diffraction,³ quasielastic helium scattering,⁴ and laser-induced thermal desorption.⁵ These methods make a macroscopic average measurement of diffusion, and the measurement may be affected by the presence of surface defects such as steps. They also do not provide information on the interactions between adsorbed atoms. Methods that observe diffusion at a more microscopic scale may overcome these limitations. Field electron emission may be used to measure diffusion by direct observation of the diffusion of an overlayer over the end of a tip as a function of temperature.⁶ Another approach is to analyze the correlations of field-emission current fluctuations generated by atoms or molecules diffusing into and out of a small area of the surface.⁷ Field ion microscopy has been extensively used to directly observe the diffusion of single atoms and small clusters on a number of metal surfaces.^{8,9} These observations al-

low a direct measurement, over a wide range of temperatures, of anisotropic diffusion, diffusion over barriers such as steps, and cooperative diffusion. In the appropriate temperature range, the scanning tunneling microscope also allows diffusion of single adatoms to be observed on a variety of systems.

Several methods have been employed for obtaining quantitative measurements of diffusion from STM images. The simplest method is to measure the change in shape of a nanometer scale feature placed on the surface.^{1,2} Another method is to observe the shape and number of islands formed during deposition of atoms on a surface¹⁰ and after annealing of the surface. These experimental results can be compared with the results of Monte Carlo simulations to determine diffusion parameters.¹¹ On other systems, the diffusion is slow enough so that the hopping of atoms can be observed directly from the changes between images taken sequentially.¹²⁻¹⁵ Diffusion occurring at rates faster than the time between two images has been observed in a number of systems,^{12-14,16,17} but obtaining a quantitative measurement of diffusion is difficult in this case. Since interpretation of the images is complicated by the possibility that the state of the surface may change between the acquisition of two image pixels, few have tried to derive quantitative information from these images. Binnig, Fuchs, and Stoll have attempted to measure a diffusion constant of oxygen on nickel from "flicker noise" or spikes in the STM tunneling current, which they interpreted as due to atoms diffusing under the tip.¹⁶ Poensgen *et al.* calculated the density and diffusion rate of kinks from the "frizziness" or apparent roughening of steps in their STM images caused by step diffusion.¹⁷ Here, the diffusion of sulfur adatoms on terraces on the Re(0001) surface is investigated.

This system has been studied previously by both STM (Refs. 18 and 19) and LEED.^{20,21} Sulfur forms four ordered structures on this surface, with (2×2) , $(3\sqrt{3} \times \sqrt{3})$, $[\frac{3}{1} \frac{1}{3}]$, and $(2\sqrt{3} \times 2\sqrt{3})R 30^\circ$ unit-cell periodicities. Dynamical low-energy electron-diffraction (LEED) calculations of sulfur on metal surfaces²² have shown that, at low coverages, sulfur bonds at the highest coordination site. On rhenium, a dynamical LEED analysis of the $p(2 \times 2)$ structure²¹ has shown that the binding site is the threefold hcp hollow site. At coverages of one-quarter monolayer and higher, STM imaging has shown stable structures on the surface, with no apparent diffusion of sulfur adatoms.¹⁸ The results presented here are at lower sulfur coverages.

II. EXPERIMENT

The experiments were performed in a standard surface science UHV chamber with a base pressure of 2×10^{-10} Torr. The chamber was equipped with Auger electron spectroscopy (AES), LEED, an Ar^+ sputtering gun, and the STM. The design of the STM is described elsewhere.²³ The single-crystal sample could be heated with an electron-beam heater, and cooled by placing the sample holder in contact with a copper block cooled by liquid nitrogen.

The rhenium crystal was cleaned in UHV by Ar^+ bombardment and cycles of heating to 1000°C in the presence of 5×10^{-7} Torr of oxygen. This treatment removed sulfur and carbon contamination. The oxygen was removed by heating the crystal to approximately 1800°C .

Once the crystal was clean, as verified by AES, it was exposed to H_2S at 5×10^{-8} Torr for 2–10 min while heating to approximately 700°C . H_2S gas decomposes on the surface, leaving behind sulfur. The crystal was then cooled to room temperature. The large-scale ordering of the sulfur overlayer was determined with LEED, and the sulfur coverage determined with AES. If the coverage was higher than desired, some sulfur could be desorbed from the surface by heating to approximately 1000°C for several seconds. Occasionally, annealing for a short period of time at 600°C was necessary to obtain an ordered LEED pattern. Sulfur coverages from about one-tenth to one-quarter of a monolayer were produced. In this coverage range, the LEED pattern was $p(2 \times 2)$. The pattern had the highest contrast at coverages near one-quarter monolayer.

III. RESULTS

STM images of the surface with a coverage of one-quarter monolayer sulfur and a $p(2 \times 2)$ LEED pattern show a triangular lattice of maxima. An example of such an image is shown in Fig. 1. Within the $\pm 10\%$ accuracy of the STM piezoelectric calibration, the maxima in these images are separated by a distance of twice the Re lattice constant a , consistent with a $p(2 \times 2)$ overlayer. The image quality appeared best at a bias voltage of ± 25 to ± 100 mV and 1 nA of tunnel current. The STM images became more noisy and the contrast was unstable outside this range. On clean surfaces, no corrugation due to the underlying Re lattice could be detected, either directly or

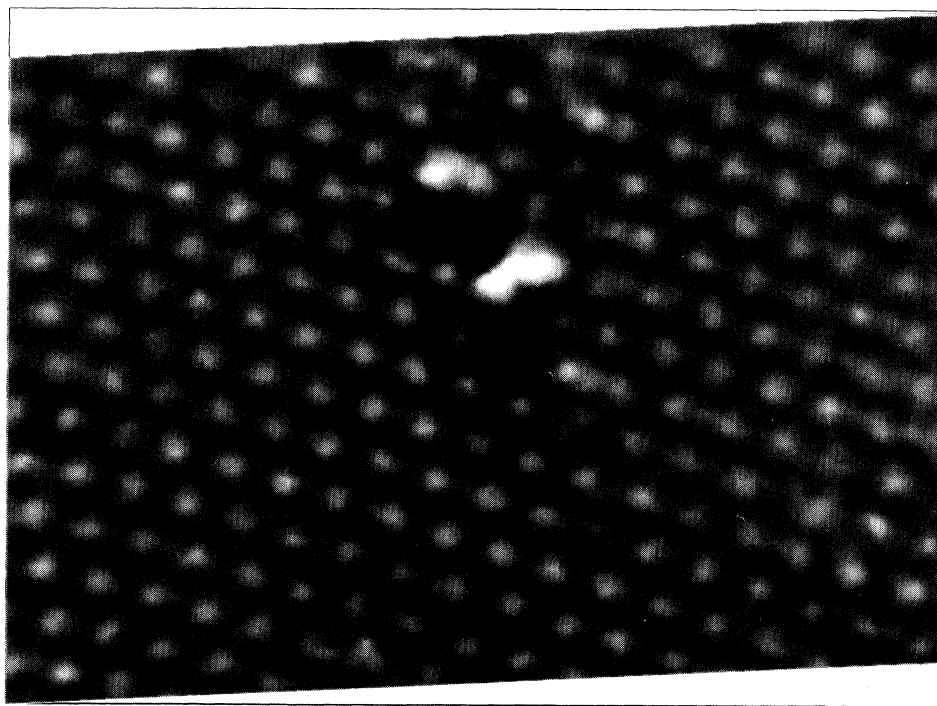


FIG. 1. STM constant-height image of a complete $p(2 \times 2)$ overlayer of sulfur on $\text{Re}(0001)$. The current maxima (bright spots) in the image are at the location of sulfur atoms, and are spaced at twice the rhenium lattice distance a , or 5.5 \AA . There is a defect in the center of the image, and a missing sulfur atom below the defect.

in the Fourier transform of the image. The corrugation of transition metals is generally very small, of the order of a few hundredths of an angstrom, and probably below the noise of our STM.

Sometimes point defects appeared in images such as Fig. 1. These always appeared as a missing current maximum, allowing the current maxima in Fig. 1 to be interpreted as being at the locations of the sulfur atoms. Sometimes the sulfur atoms appeared as triangular- or Y-shaped maxima. We have been able to attribute the changes in image contrast to changes in the structure of the STM tip, and connect each image appearance to a particular structure of the tip.²⁴ These tip changes occurred randomly and at intervals varying from a few seconds to several minutes. Our image acquisition time is typically 20 sec in the present experiments.

At lower coverages, the surface was covered with islands of the $p(2 \times 2)$ structure, such as the one shown in Fig. 2. The islands varied in size between approximately 4 and 20 atoms. The presence of $p(2 \times 2)$ islands at very low sulfur coverages indicates that the interaction between single sulfur atoms, mediated by the substrate, is attractive at the third-nearest-neighbor distance of twice the rhenium lattice constant ($2a$), and less attractive or repulsive at nearest-neighbor (a) and second-nearest-neighbor ($\sqrt{3}a$) distances. The distances between neighboring hcp hollow sites are shown in Fig. 3.

There are two unusual features of the images of $p(2 \times 2)$ sulfur islands. First, in smoothed images, such as Fig. 2, the corrugation of the sulfur atoms making up the islands is not constant. Atoms near the center of the is-

lands have the highest corrugation, while those near the edge have a lower corrugation. Second, the raw data images, such as Fig. 4, contain a large amount of apparent noise in the areas between the islands. This noise is primarily made up of horizontal dashes, which extend approximately the width of an atom in the horizontal direction, but only one to three lines in the vertical direction.

These features of the images may be explained as an effect of sulfur atoms moving across the surface at a time scale shorter than that required to produce a STM image. The STM tip rasters across the surface in the horizontal direction while scanning slowly in the vertical direction. Therefore, adjacent pixels in the horizontal direction are acquired much closer together in time than adjacent pixels in the vertical direction. If the diffusion rate is not too rapid, a diffusing atom has much less probability of moving while it is being scanned over in one line than it does between scan lines. The images of atoms are, therefore, complete in the horizontal direction, but not in the vertical direction. These incomplete images of atoms are shaped like horizontal dashes. Images with features of this type have been observed before,^{12-14,17} and they were also interpreted as diffusing atoms or molecules.

The decrease in the corrugation of the atoms at the edges of islands seen in smoothed images can be explained as a result of diffusion. The Fourier filtering used to remove noise from the images spatially smooths the image, blending each scan line into the adjacent ones. If an atom is only present in half of the lines in the raw data, it will appear in all lines in the filtered image, but with a lower corrugation. The atoms at the edges of is-

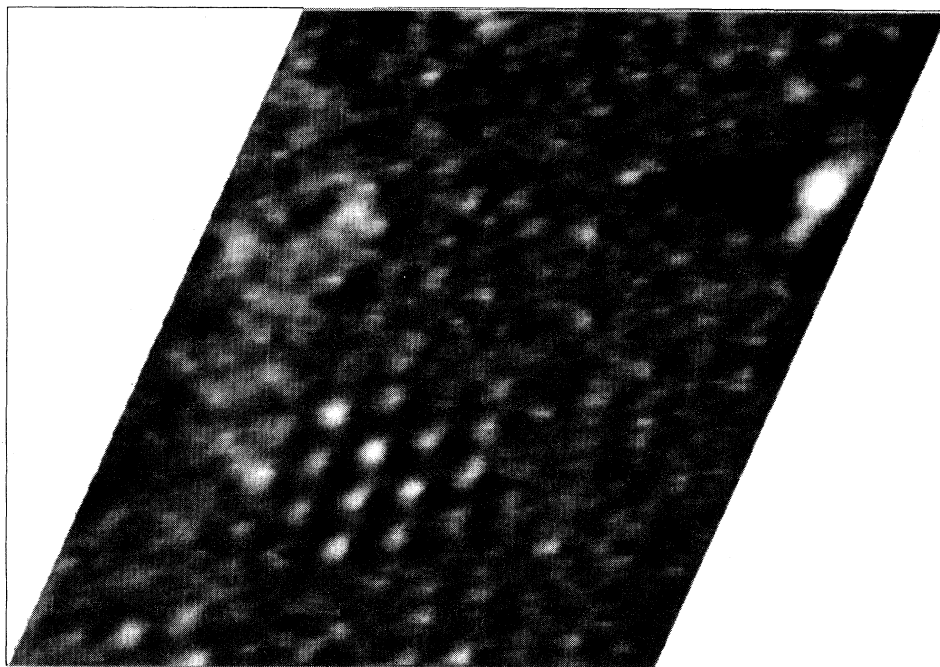


FIG. 2. Fast-Fourier-transform filtered STM image of sulfur islands which form at low coverage. The corrugation of the atoms on the islands is higher at the center than at the edge. This is explained by the reduced residence time of the sulfur atoms at the edge of the island.

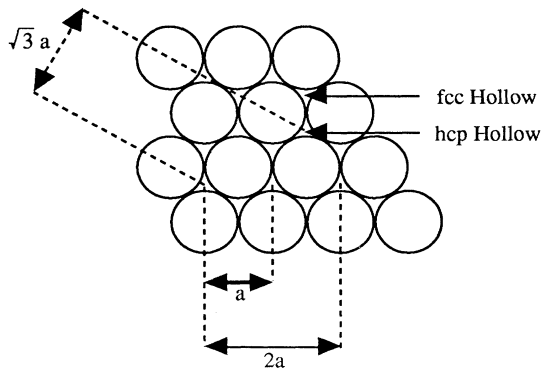


FIG. 3. Diagram showing the distances between nearest-neighbor hcp hollow sites on the Re(0001) surface. The fcc and hcp hollow sites are labeled.

lands are clearly more likely to diffuse than those at the center, and therefore they have a lower corrugation, due to a lower percentage occupation of these lattice sites. Atoms at the center of islands are blocked from moving by their neighbors. In contrast, atoms at the edges of islands are free to move away from the island, but weakly attracted to the island by the attractive interaction between the sulfur atoms at the $2a$ distance.

In any measurement of diffusion by STM, it is important to consider what effect, if any, the presence of the

STM tip may have on the process. Could the presence of the STM tip over the surface be catalyzing or increasing the rate of diffusion? There are several reasons to believe that this is unlikely. First, there is no evidence in the images that the tip is having any direct effect. Two images, one in which the tip is scanning to the right in each image line and one with it scanning left, are acquired simultaneously. We found them to be identical. If the tip were pushing the sulfur atoms in the scan direction, the motion would be apparent from large differences in the position of sulfur atoms in these two images.

Second, at the gap used in imaging, approximately $50 \text{ M}\Omega$, theoretical calculations of the tunneling gap show that the tip is 6 \AA from the sulfur atoms on the surface.²⁴ This distance is too long for any direct chemical bond between the sulfur atoms and the tip-end atom. Experimentally, Stroscio and Eigler have shown that a gap resistance ten times as small as the one used here is required to move xenon atoms along the rows on Ni (110), and a gap 250 times as small is needed to move platinum atoms on the Pt (111) surface.²⁵ The binding energy of sulfur to the rhenium surface is more than an order of magnitude stronger than that of xenon on nickel, and of the same order of magnitude as platinum on platinum. Therefore the gap resistance used in imaging is several orders of magnitude larger than that needed to push the sulfur atoms across the surface.

Naturally, sulfur would not be expected to diffuse

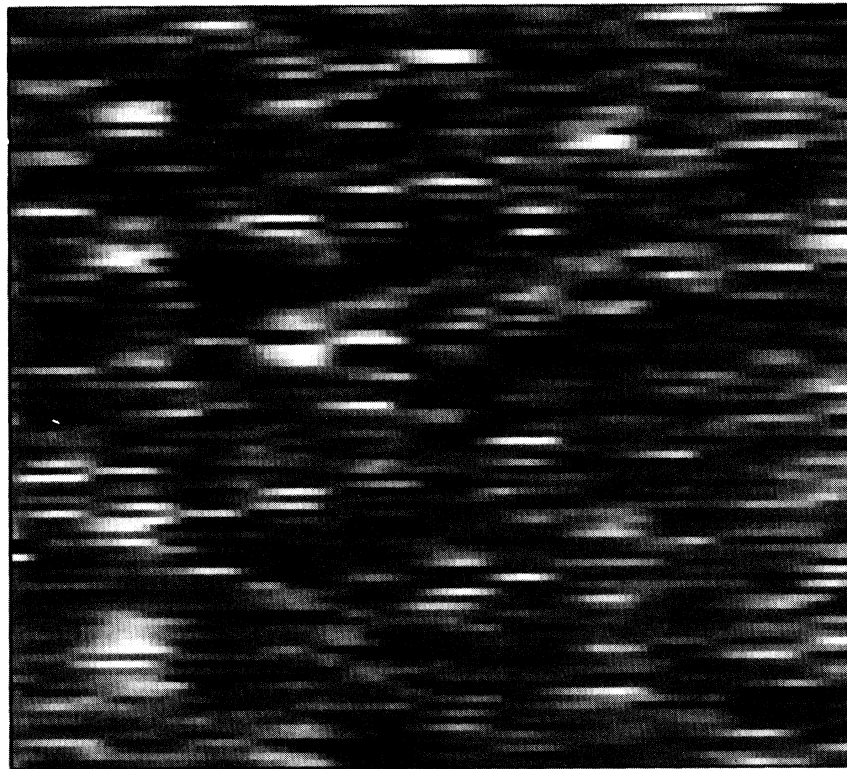


FIG. 4. STM image showing the raw data image of an area between (2×2) islands. Horizontal dashes in the image are the fraction of a sulfur atom that is imaged before it moves to another site.

smoothly over the surface. Because the hcp hollow sites have a lower energy than other sites, the sulfur will occupy these sites most of the time, and hop between them as a lattice gas.²⁶ While direct evidence showing that the sulfur diffuses as a lattice gas will be presented later, there is some evidence of this in the raw data. In some areas of the images, such as Fig. 4, it is possible to observe streaks due to single atoms hopping between hcp hollow sites. Here the dashes in the image appear at one point in the section of the image lines, but never at more than one.

The results so far show that there are sulfur atoms diffusing over the surface as a lattice gas in the areas between islands of $p(2 \times 2)$ ordered sulfur. There are more questions about how this diffusion occurs that may be answered with the STM data: What is the residence time of a sulfur atom per site? What is the energy barrier for diffusion? How do the diffusing sulfur atoms interact with each other?

IV. CORRELATION FUNCTION

In order to answer these questions, a method for interpreting STM images of diffusing atoms needs to be developed. As some of the sulfur adatoms are moving at a rate faster than the STM imaging, it is impossible to know the exact location and motion of all atoms in the image. However, the average positions of atoms relative to each other is contained in the image data. A spatial pair-correlation function was used to extract this information. This function is the average product of the tunnel current value at pixels in an image or part of an image separated by a particular vector,

$$C(\mathbf{r}, t) = \frac{1}{N} \sum_{\mathbf{r}_0} I(\mathbf{r}_0, t_0) I(\mathbf{r}_0 + \mathbf{r}, t_0 + t), \quad (1)$$

where N is the number of products in the sum, and $I(\mathbf{r}, t)$ is the current value at a pixel in the image at position \mathbf{r} at time t . In a STM image, t is a function of \mathbf{r} , since it is only possible for the tip to be at one point in the image at a time. The value of this average product or correlation function is a measure of how well pixels at a particular distance and time separation are correlated. On a well-ordered surface, pixels separated by vectors close to the lattice vectors of the overlayer should be well correlated, because the overlayer atoms are well correlated at this distance. This spatial correlation function can be represented as a two-dimensional map or image, which we will call a correlation image.

It is convenient to express the tunneling current as

$$I(\mathbf{r}, t) = I_0 + I_n(t) + \sum_i n_i(t) f(|\mathbf{R}_i - \mathbf{r}|), \quad (2)$$

where $I_0 + I_n(t)$ is an average current and noise, and the sum represents the contribution of the sulfur overlayer. It is over the lattice of hcp hollow sites \mathbf{R}_i , where the occupation $n_i(t)$ is 0 or 1, depending on whether or not a site is occupied at time t . The function f describes the shape of sulfur atoms in the image.

Substituting this model for the current into Eq. (1), one

finds that only one term besides the noise is not constant. The noise term averages to zero for sufficiently large times t . The remaining term is the average correlation between atoms at two times and places separated by a fixed time and distance,

$$I_{\text{corr}}(\mathbf{r}, t) = \sum_{ij} \langle n_i(t_0) n_j(t_0 + t) \rangle_{t_0} \times \langle f(|\mathbf{r}_0|) f(|\mathbf{R}_j - \mathbf{R}_i - \mathbf{r}_0 - \mathbf{r}|) \rangle_{\mathbf{r}_0}. \quad (3)$$

One would expect that the correlation function has a maximum at each vector \mathbf{r} which is a lattice vector separating two hcp hollow sites. The size of this maximum is proportional to the probability of overlayer atoms being separated by this lattice vector. The first term in the sum of Eq. (3) represents the separation in time at which the correlation is determined. For a STM image, one is limited to a given t for each vector \mathbf{r} , but since lattice vectors rotated by 60° are equivalent, several time separations for each lattice vector are available in the data.

In the first part of the analysis, the time correlation in Eq. (3) is neglected, and the occupations n_i and n_j are assumed to be constant in time. This is the idealized case, in which the STM image is taken quickly enough so that no adsorbate atoms move during the image acquisition. The effect of changes in n_i and n_j with time during imaging, and the information which may be obtained from these changes, will be discussed later.

The correlation function was calculated for a number of experimental images and sections of experimental images. Two representative correlation images, together with the original data, are shown in Figs. 5 and 6. When an image with many of the horizontal dashes of diffusing atoms is used as input, the correlation image shows that the surface is unexpectedly well ordered. The image shows clearly that the sulfur is diffusing between low-energy sites as a lattice gas. The correlation image has maxima on a $p(2 \times 2)$ lattice, not the (1×1) lattice of hcp hollow sites that would be expected if the sulfur atoms were not interacting. The diffusing sulfur atoms are most likely to be separated by lattice vectors of the $p(2 \times 2)$ lattice, even when they are separated by many lattice constants. At small odd multiples of a , there are minima in the correlation plot, signifying that it is unlikely to have atoms separated by this distance. The first of these minima is the lowest, due to the repulsive interaction of sulfur atoms at this short distance. Although the atoms are diffusing, they maintain a local $p(2 \times 2)$ order that extends at least several unit cells over the surface. This order is maintained even on parts of the surface, such as the upper part of Fig. 6, where there appear to be no stationary sulfur atoms.

The size of the maxima in the correlation image, as a function of their position away from the center, is a direct measure of the probability that atoms are spaced by that particular lattice vector. The experimental curve in Fig. 7 shows a cross section through several of the maxima of a correlation image. The central maximum is the correlation of each atom with itself. Each atom of the surface contributes to this peak, and thus its height is proportional to the coverage. Peaks at a distance of $2a$

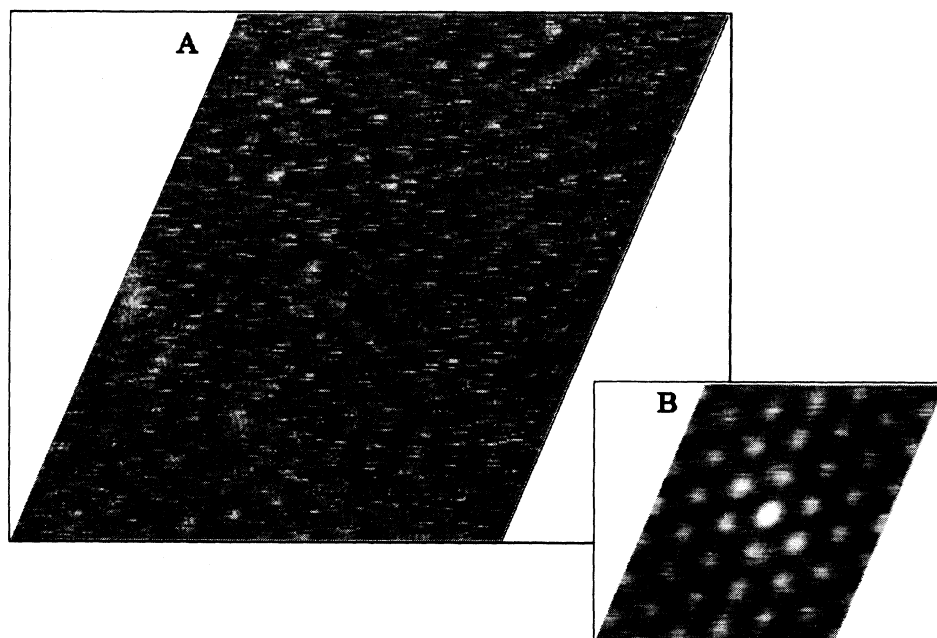


FIG. 5. A 70×70 -Å STM image (A) of diffusing sulfur atoms and the corresponding correlation image (B). The correlation image shows that the diffusing sulfur is a lattice gas that maintains a local $p(2 \times 2)$ order over several lattice distances.

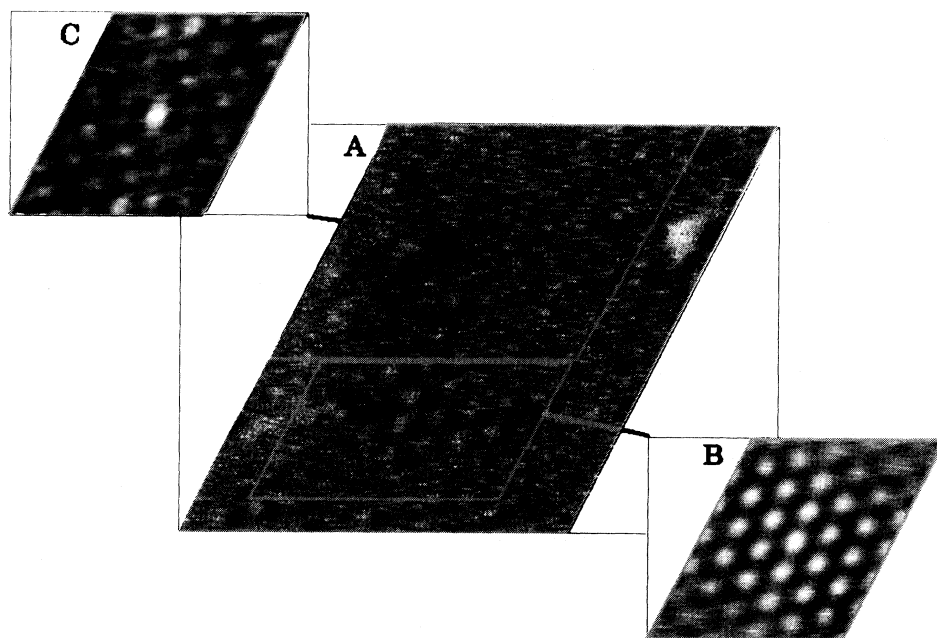


FIG. 6. STM image (A) of a sulfur island surrounded by an area of diffusing sulfur. In the correlation image (B) of the island area, all the peak heights are roughly equal. However, in the correlation image (C) of the diffusing atoms, the center peak is much higher than the surrounding peaks because the coverage in this area is low. The diffusing atoms are ordered in a $p(2 \times 2)$ overlayer lattice. The center peak of the correlation image (C) is not round due to the short residence time of sulfur atoms on one site in the low-coverage upper area of the STM image.

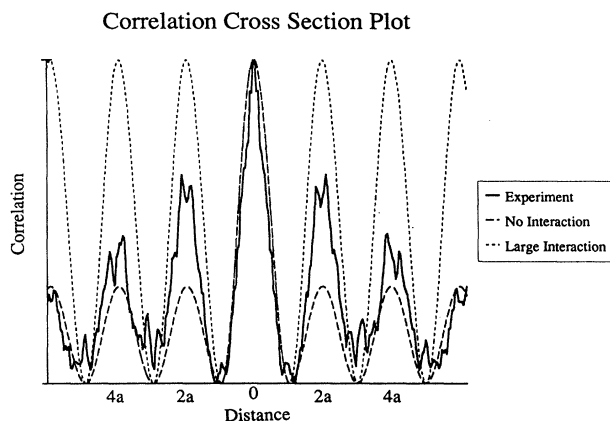


FIG. 7. Cross section of a correlation image and the expected cross section in the two limiting cases of no interaction (dashed line) and a large interaction (dotted line) between sulfur atoms. In both cases, the sulfur atoms are assumed to be only on a $p(2 \times 2)$ overlayer lattice, as found experimentally. The experimental cross section is between the two limits.

receive a contribution from each pair of atoms separated by $2a$ in the image. Their height is proportional to the probability of $2a$ neighbors on the overlayer lattice. Peaks at large distances represent the probability of finding two atoms at a large distance from each other at the same time. Since atoms far from each other should not be well correlated, and since the probability of each atom being present is proportional to the coverage, this peak height is proportional to the square of the coverage.

V. SULFUR-SULFUR INTERACTION ENERGY

The ability to measure the relative probability of atoms being separated by different distances on the surface allows the interaction of the atoms to be measured by fitting the results to a model. The most basic information available in the correlation function is the sulfur coverage and the probability of pairs of atoms at the $2a$ distance on the rhenium surface. If there were no interaction between overlayer atoms, the probability of pairing at multiples of $2a$ would be the square of the coverage for any separation distance, as indicated by the dashed curve in Fig. 7. If there is an attractive interaction between atoms separated by this distance, one would expect an increased number of pairs. In the limiting case, in which the attraction is so strong that all the sulfur atoms are on islands, a cross section of the correlation image would appear like the dotted line in Fig. 7. The actual experimental data are in between the two limits.

The number of pairs can be calculated in a simple model. We chose to use the simplest possible model for the interaction between the diffusing sulfur atoms, an Ising model,²⁷ since it may be solved analytically. In this model, atoms are only allowed to be on the sites of a lattice, in this case the $p(2 \times 2)$ overlayer lattice. This accurately reflects the experimental finding that repulsive interactions prevent sulfur atoms from coming closer together than $2a$ at the low sulfur coverage of the experiment.

The model only includes the interaction between pairs of atoms separated by $2a$. However, this interaction appears to dominate the long-range adsorbate-adsorbate interactions. The lack of ordered structures with sulfur atoms separated by more than $2a$ is evidence that longer-range interactions are weaker than the $2a$ -separated pair interaction. While, at higher coverages, many-body interactions must be considered to explain the variety of structures formed by sulfur on rhenium,¹⁸ the atoms are widely separated at the low coverage of the $p(2 \times 2)$ structure, so interactions beyond the nearest neighbor are not likely to be significant. Therefore the Ising model is a reasonable approximation for the experimental system.

In our model, the total energy is the sum of a pair-interaction energy and a chemical potential energy for each atom. The total pair-interaction energy is simply the product of a pair-interaction energy E_{12} and the number of pairs separated by a distance of $2a$. The chemical potential-energy term controls the equilibrium coverage. The total energy of the system may be written as

$$H = E_{12} \sum_{\text{pairs}(i,j)} n_i n_j + E_1 \sum_i n_i, \quad (4)$$

where n_i is the occupation of a site i . This model is analogous to the Ising model for ferromagnetism.²⁸ The first term is equivalent to the exchange interaction between pairs of spins, and the second term is equivalent to the interaction between spins and a magnetic field. Equation (4) may be rewritten in the usual Ising form by substituting the spin σ_i for the occupation,

$$n_i = \frac{1}{2}(1 + \sigma_i). \quad (5)$$

This model may be solved analytically using the Weiss molecular-field approximation.²⁷ Since the Re(0001) surface is a triangular lattice, the calculation was done on a group of three overlayer nearest-neighbor sites. All the other nearest neighbors of these atoms on the overlayer were taken to have the average occupation. The probability of pairs was calculated as a function of average coverage and pair-interaction energy E_{12} , and normalized to the noninteracting case, where the probability is equal to the square of the coverage.

The results of this model are shown in a contour graph, Fig. 8, of pair-interaction energy as a function of coverage and normalized pair probability. The experimental results from the correlation function are also shown as points. From the fit of the experimental results to the theoretical curves, the pair-interaction energy for sulfur atoms is found to be 24 ± 5 meV. The error bars on the data are wide because there are statistical fluctuations due to the limited size of the STM images.

The molecular-field approximation assumes that the overlayer is homogeneous, which is inaccurate when large islands form in the overlayer. This approximation is valid at low coverages and energies, but causes an underestimate of the probability of pairs at higher energies and coverages. An exact solution of the Ising model,²⁹ which is possible only at a coverage of one-eighth of a monolayer, shows that islands will form in the overlayer for interactions above 28 meV at room temperature.

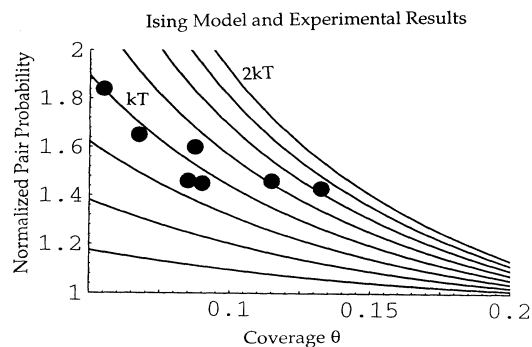


FIG. 8. Graph of the results of the Ising model and experimental data. The horizontal axis represents the sulfur coverage or the ratio of the number of sulfur atoms to first-layer rhenium atoms. The vertical axis is the probability of pairs of atoms at the $2a$ distance. This axis is normalized such that the result is one in the zero-interaction energy case in which pairs form randomly. The results of the Ising model are displayed as contours of constant interaction energy spaced at intervals of $0.25 kT$. The experimental results are shown as dots. The five experimental points at low coverage follow these contours, but the contours fall below the two higher-coverage points due to inaccuracies in the theoretical model at high coverage. From the fit of the five low-coverage experimental points to the Ising model, the attractive interaction energy between sulfur atoms at the $2a$ distance was determined to be 24 ± 5 meV.

Since this energy is very close to the interaction energy determined by this experiment, the model is not accurate for this system at coverages above approximately one-eighth of a monolayer. Due to this limitation of the theoretical model, the two highest-coverage experimental points do not fit well with the model and were not used in the determination of the interaction energy.

The effect of the approximation that the time part of the correlation in Eq. (3) is ignored must be considered. Since atoms are known to be moving at a rate comparable to the scan speed, this term is clearly of some significance. However, its presence does not affect the size of the central maximum or maxima at large distances in the correlation image. At the central maximum, the time difference is nearly zero, so the approximation that n_i and n_j are constant is nearly valid. At large distances, there is little spatial correlation, so the expected lack of time correlation is unimportant. However, the probability of pairs separated by $2a$ would be affected by this term. If the diffusion rate is too fast, there is a large chance of one or both atoms in a pair moving before the tip scans over them both. This would cause a decrease in the measured probability of pairs. In the limiting case of short residence time, these maxima would be the same size as those at large distances, and proportional to the square of the coverage. However, the amount of the decrease would be dependent on the time separation between the tip scanning over each of the two atoms, and so it would be dependent on the angle of the pair relative to the horizontal scan direction. Within the measurement error, no such dependence was seen in the experimental results.

This may be due to the increase in the residence time caused by the attractive pair interaction. Since none of the correlation maxima in the image is strongly affected, inaccuracies due to the constant $n_i(t)$ approximation are expected to be small.

The time-correlation term does have an effect on the shape of the central maximum in areas of the surface with a very low sulfur coverage, such as the upper part of Fig. 6. In these areas, the sulfur atoms appear to move before they are completely imaged. The time correlation in Eq. (3) decays with increasing time separation, as the atoms have an increasing probability of having moved. This causes a decay in the central maximum of the correlation image in the y -scan direction. Comparison of the central maximum in the correlation of the low-coverage section of Fig. 6 with that of the island shows that the asymmetric shape is not due to the STM tip structure.

VI. COMPARISON WITH THEORY

The residence time for atoms that are not attached to an island can be determined from the shape of the maxima in the correlation image, or from the size in the y -scan direction of the dashes in the raw data. This turns out to be approximately two STM scan lines, or 100 msec. An estimate of the energy barrier to diffusion can be calculated from this measurement. Since the residence time was measured at only one temperature, the exact preexponential term cannot be determined. Using a standard preexponential of 10^{14} sec^{-1} , the mean number of diffusions per second between two sites is given by the Einstein equation:³⁰

$$n = 10^{14} \exp \left[- \frac{E}{kT} \right]. \quad (6)$$

Taking into account the number of possible sites to which an atom may diffuse, this formula gives a diffusion energy barrier of 0.79 ± 0.1 eV. Since the residence time and preexponential factor determine E through a logarithmic dependence, errors of one order of magnitude in these parameters imply only a 0.06-eV change in E .

This result compares well with the energy barrier predicted by an extended Hückel calculation of the relative energy of a sulfur atom at several positions on a rhenium cluster. We performed such a calculation by placing a sulfur atom on the top of a three-layer-thick, 70-atom cluster of rhenium atoms at hcp and fcc hollow sites, the top site, and a bridge site. The height of the sulfur atom was such that its distance to the nearest rhenium atom was set equal to the sum of the covalent radii. A correction was made for the effect of the edges of the cluster.³¹ Relative to the hcp hollow site, the fcc hollow had an energy of 0.1 eV, the bridge site had an energy of 0.74 eV, and the top-site energy was 1.6 eV. Therefore, the lowest-energy path between two hcp hollow sites is over a bridge site to a fcc hollow and then over a second bridge site. The highest energy along this path is at the bridge sites. The energy of these sites (0.74 eV) compares quite well to the experimentally determined energy barrier.

This result is toward the high end of the range of

diffusion barriers that have been measured by field ion microscopy, especially on close-packed surfaces. In particular, the energy barrier for diffusion of sulfur on Ni (111) has been measured to be 0.29–0.30 eV.³² However, this discrepancy can be explained by the large binding energy of sulfur on Re(0001). Diffusion barriers roughly scale with adsorption energy. The adsorption energy of sulfur on Re(0001) of 4.3 eV (Ref. 20) is approximately 65% higher than that of sulfur on Ni of 2.6 eV.³³

VII. CONCLUSION

We have demonstrated the application of STM to study diffusion on individual adatoms on a surface, even when the diffusion time is small compared to the imaging time. The usefulness of a spatial correlation function to extract quantitative information from the diffusion images was shown. Quantitative results for the interactions

between the diffusing atoms and the diffusion energy could be determined from the data. STM studies of diffusion would be even more informative if the temperature of the system could be varied. This was not possible in this experiment, but instruments that allow imaging at variable temperatures are available. Using some of the analysis methods used here would allow phenomena such as surface diffusion and phase transformations to be studied in great detail.

ACKNOWLEDGMENTS

This work has been supported by the Director, Office of Energy Research, Office of Basic Energy Sciences, Materials Science Division of the U.S. Department of Energy, under Contract No. DE-AC03-76SF00098. P.S. acknowledges the support of NATO. O.D. acknowledges the support of the KFUPM Research Committee.

*Permanent address: Laboratoire de Chimie Théorique, ENS Lyon 46, allée d'Italie, 69464 Lyon CEDEX 07, France; and Institut de Recherche sur la Catalyse, 2, Avenue A. Einstein, 69626 Villeurbanne CEDEX, France.

†Permanent address: University Of Petroleum and Minerals, Dhahran, Saudi Arabia.

¹D. A. Sommerfeld, R. T. Cambron, and T. P. Beebe, Jr., *J. Phys. Chem.* **94**, 8926 (1990).

²D. J. Trevor and C. E. D. Chidsey, *J. Vac. Sci. Technol. B* **9**, 964 (1991).

³J. H. Neave, B. A. Joyce, P. J. Dobson, and N. Norton, *Appl. Phys. A* **31**, 1 (1983).

⁴B. J. Hinch, J. W. M. Frenken, G. Zhang, and J. P. Toennies, *Surf. Sci.* **259**, 288, (1991).

⁵S. M. George, A. M. DeSantolo, and R. B. Hall, *Surf. Sci. Lett.* **159**, L425 (1985).

⁶R. Gomer, *Field Emission and Field Ionization* (Harvard University Press, Cambridge, MA, 1961).

⁷R. Gomer, *Surf. Sci.* **38**, 373 (1973).

⁸T. Tsong, *Rep. Prog. Phys.* **51**, 759 (1988).

⁹G. Ehrlich and K. Stolt, *Annu. Rev. Phys. Chem.* **31**, 603 (1980).

¹⁰Y.-M. Mo, R. Kariotis, B. S. Swartzentruber, M. B. Webb, and M. G. Lagally, *J. Vac. Sci. Technol. A* **8**, 201 (1990).

¹¹H. B. Elswijk, A. J. Hoeven, E. J. van Loenen, and D. Dijkkamp, *J. Vac. Sci. Technol. B* **9**, 451 (1991).

¹²R. M. Feenstra, A. J. Slavin, G. A. Held, and M. A. Lutz, *Phys. Rev. Lett.* **66**, 3257 (1991).

¹³Chr. Günther and R. J. Behm (unpublished).

¹⁴V. M. Hallmark, S. Chiang, J. K. Brown, and Ch. Wöll (unpublished).

¹⁵E. Ganz, S. K. Theiss, I. S. Hwang, and J. Golovchenko, *Phys. Rev. Lett.* **68**, 1567 (1992).

¹⁶G. Binnig, H. Fuchs, and E. Stoll, *Surf. Sci. Lett.* **169**, L295 (1986).

¹⁷M. Poensgen, J. F. Wolf, J. Frohn, M. Giesen, and H. Ibach, *Surf. Sci.* **274**, 430 (1992).

¹⁸R. Q. Hwang, D. M. Zeglinski, D. F. Ogletree, A. Lopez Vazquez-de-Parga, G. A. Somorjai, and M. Salmeron, *Phys. Rev. B* **44**, 1914 (1991).

¹⁹D. F. Ogletree, R. Q. Hwang, D. M. Zeglinski, A. Lopez Vazquez-de-Parga, G. A. Somorjai, and M. Salmeron, *J. Vac. Technol. A* **9**, 886 (1991).

²⁰D. G. Kelly, A. J. Gellman, M. Salmeron, G. A. Somorjai, V. Maurice, H. Huber, and J. Oudar, *Surf. Sci.* **204**, 1 (1988).

²¹D. Jentz, G. Held, M. A. Van Hove, and G. A. Somorjai (unpublished).

²²J. M. MacLauren, J. B. Pendry, P. J. Rous, D. K. Saldin, G. A. Somorjai, M. A. Van Hove, and D. D. Vvedensky, *A Handbook of Surface Structures* (Reidel, Dordrecht, 1987).

²³D. M. Zeglinski, D. F. Ogletree, T. P. Beebe, Jr., R. Q. Hwang, G. A. Somorjai, and M. Salmeron, *Rev. Sci. Instrum.* **61**, 3769 (1990).

²⁴J. C. Dunphy, D. F. Ogletree, M. Salmeron, P. Sautet, M.-L. Bocquet, and C. Joachim, *Ultramicroscopy* **42-44**, 490 (1992).

²⁵J. A. Stroscio and D. M. Eigler, *Science* **254**, 1319 (1991).

²⁶T. Ala-Nissila and S. C. Yang, *Phys. Rev. Lett.* **65**, 879 (1990).

²⁷F. Reif, *Statistical and Thermal Physics* (McGraw-Hill, New York, 1965), pp. 428–434.

²⁸T. L. Einstein, *Langmuir* **7**, 2520 (1991).

²⁹J. Stephenson, *J. Math. Phys.* **5**, 1009 (1964).

³⁰A. Zangwill, *Physics at Surfaces* (Cambridge University Press, Cambridge, England, 1988), p. 362.

³¹P. Sautet and J.-F. Paul, *Catal. Lett.* **9**, 245 (1991).

³²G. L. Kellogg, *J. Chem. Phys.* **83**, 852 (1985).

³³J. G. McCarty and H. Wise, *J. Chem. Phys.* **72**, 6332 (1980).

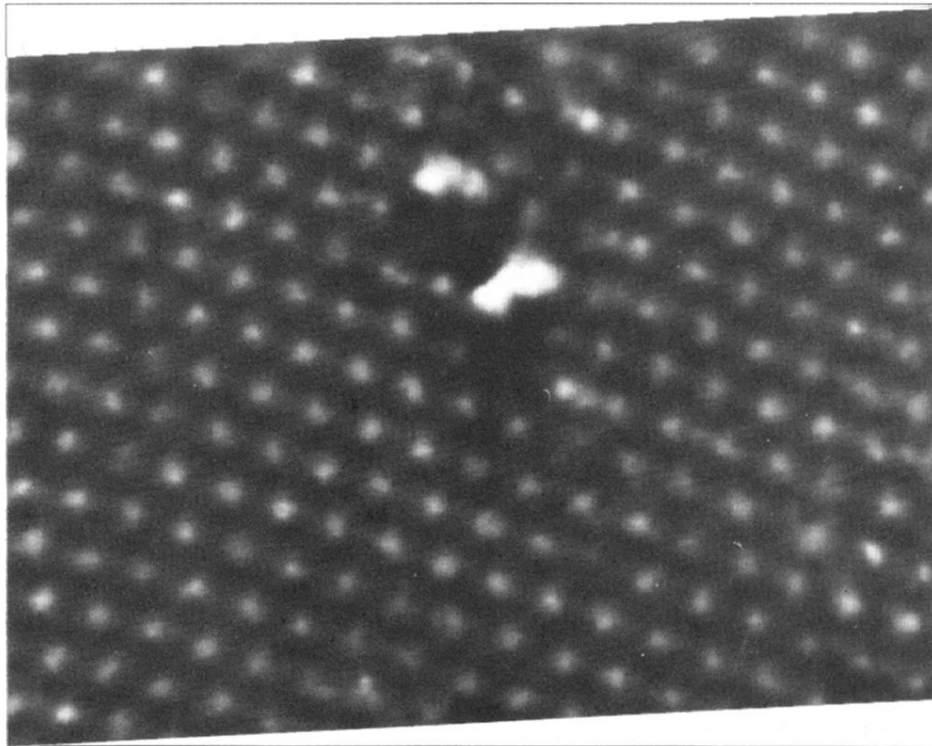


FIG. 1. STM constant-height image of a complete $p(2 \times 2)$ overlayer of sulfur on Re(0001). The current maxima (bright spots) in the image are at the location of sulfur atoms, and are spaced at twice the rhenium lattice distance a , or 5.5 Å. There is a defect in the center of the image, and a missing sulfur atom below the defect.

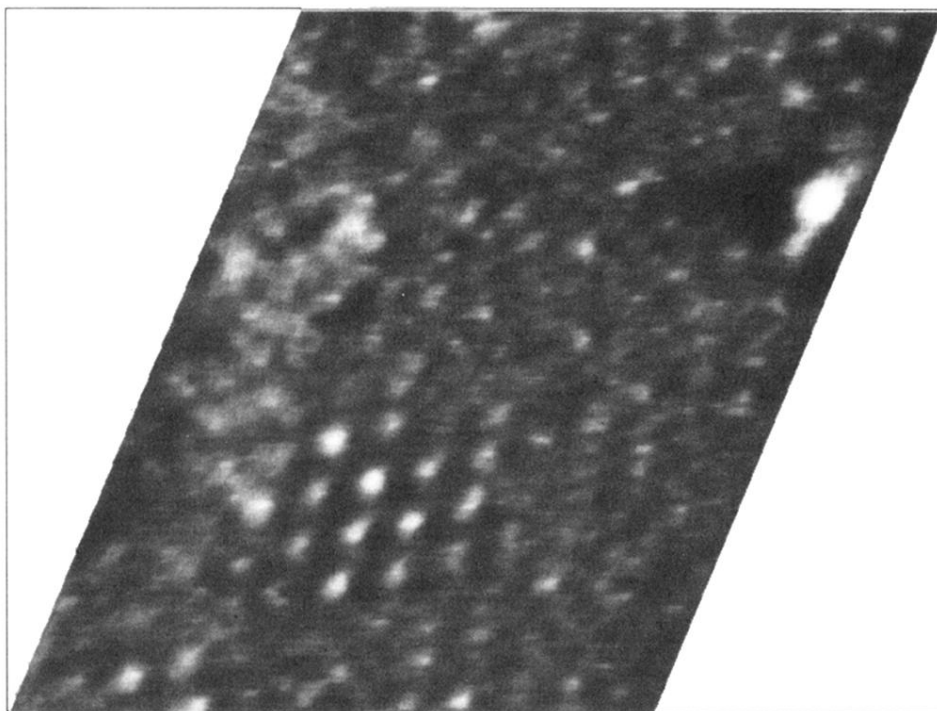


FIG. 2. Fast-Fourier-transform filtered STM image of sulfur islands which form at low coverage. The corrugation of the atoms on the islands is higher at the center than at the edge. This is explained by the reduced residence time of the sulfur atoms at the edge of the island.

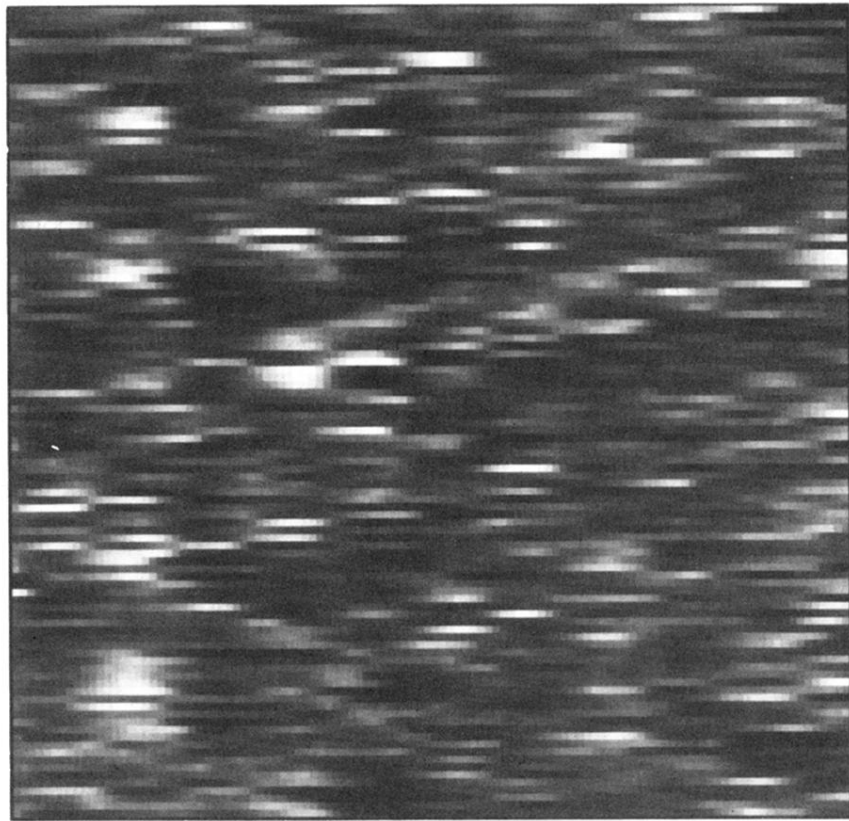


FIG. 4. STM image showing the raw data image of an area between (2×2) islands. Horizontal dashes in the image are the fraction of a sulfur atom that is imaged before it moves to another site.

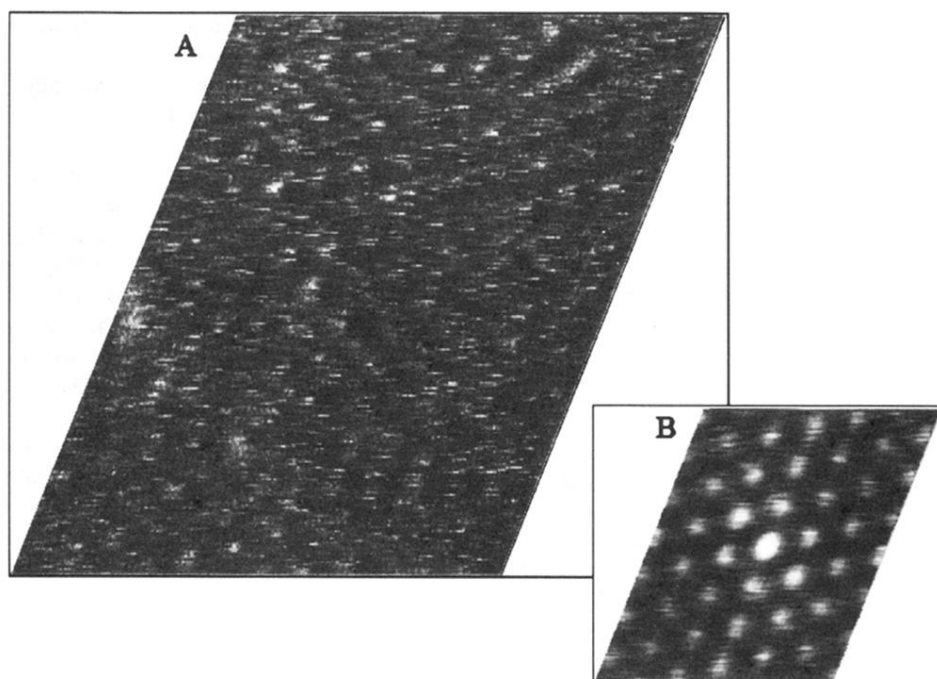


FIG. 5. A 70×70 -Å STM image (A) of diffusing sulfur atoms and the corresponding correlation image (B). The correlation image shows that the diffusing sulfur is a lattice gas that maintains a local $p(2 \times 2)$ order over several lattice distances.

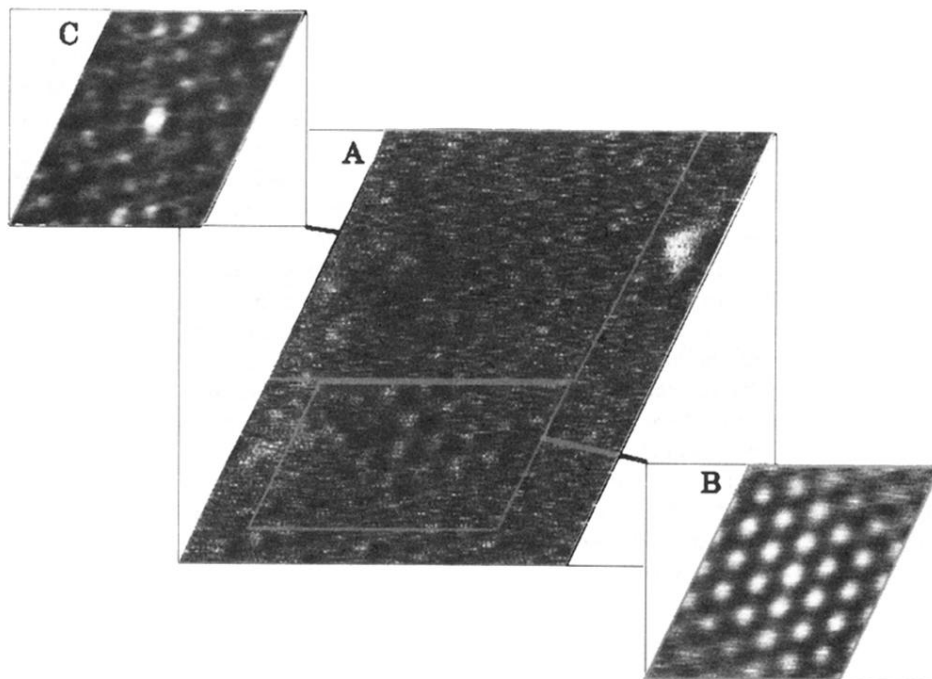


FIG. 6. STM image (A) of a sulfur island surrounded by an area of diffusing sulfur. In the correlation image (B) of the island area, all the peak heights are roughly equal. However, in the correlation image (C) of the diffusing atoms, the center peak is much higher than the surrounding peaks because the coverage in this area is low. The diffusing atoms are ordered in a $p(2 \times 2)$ overlayer lattice. The center peak of the correlation image (C) is not round due to the short residence time of sulfur atoms on one site in the low-coverage upper area of the STM image.